VISTA: Exploring Vertiport Site Selection with Visual Analytics

Haipeng Zeng, Wei Huang, Xingyu Zhu, Yanqing Peng, Wenjie Shi, Quan Li and Shaorui Zhou

***Abstract*—The rapid development of electric vertical takeoff and landing (eVTOL) technology is transforming urban air mobility (UAM), offering a promising solution for alleviating ground traffic congestion. However, the successful integration of eVTOLs into urban environments depends on the careful selection of vertiports, which must meet strict safety, operational, and environmental criteria. Traditional site selection methods often inadequately address the integration of three-dimensional spatial constraints into multi-criteria decision frameworks while simultaneously involving laborious repetitive workflows during location optimization processes. We present *VISTA*, a visual analytics framework designed to address these challenges. *VISTA* combines advanced 3D spatial analysis, multi-criteria decision-making, and interactive visualization tools to support informed decision-making in eVTOL site selection. By enabling users to explore and evaluate potential sites intuitively, *VISTA* facilitates the identification of the most suitable locations while balancing competing factors such as safety, accessibility, environmental impact, and cost. Further, *VISTA* allows users to iteratively adjust site selection based on localized constraints, while extrapolating these insights to broader, citywide planning considerations. Two case studies, along with expert interviews and a user study, demonstrate the practical application of *VISTA* in urban environments, highlighting its potential to streamline eVTOL deployment and enhance urban air mobility planning.**

***Index Terms*—eVTOL, Vertiport Siting, Visual Analytics**

I. Introduction

THE rapid advancement of electric vertical take-off and landing (eVTOL) technology has ushered in a new era of urban air mobility (UAM). As an innovative mode of aerial transport, eVTOL is reshaping traditional urban transportation systems. In the "air taxi" operating scenario, passengers book flights via a mobile app or platform, set their origin and destination, and then proceed to a designated vertiport for boarding. Using eVTOL technology, the aircraft bypasses ground congestion, ascends quickly, and flies to the destination before performing a precise landing at the target vertiport or designated landing point.

However, the successful integration of eVTOL into urban environments hinges on selecting appropriate vertiports. Rajendran et al. [1] identified this as one of the primary challenges for Urban Air Mobility (UAM) due to its long-term implications for infrastructure investment and operational efficiency. Existing research predominantly employs Geographic Information Systems (GIS) and Multi-Criteria Decision Analysis (MCDA) for two-dimensional spatial analysis, evaluating factors such as population density, proximity to transportation hubs, and land use [2], [3] to maximize economic benefits and reduce travel costs. Recently, Jiang et al. [4] further applied machine learning algorithms to dynamically optimize site selection decisions.

Despite these advances, large-scale deployment of vertiports continues to face significant challenges: **(1) Incorporating 3D Constraints into Multi-criteria Planning**: Traditional methods struggle to systematically integrate diverse considerations such as safety, accessibility, cost, and environmental impact within a data-driven decision-making framework. More critically, they often overlook complex three-dimensional spatial constraints inherent in low-altitude urban airspace (e.g., building heights, terrain variations, airspace regulations), frequently leading to suboptimal site recommendations. **(2) Enabling Effective User-Involved Decision Support**: Existing methods still lack interactive and visual tools that empower diverse stakeholders including urban planners, regulators, and eVTOL operators to engage in the decision-making process [5], making it difficult to dynamically adjust criteria, explore trade-offs, and visually reason about complex spatial relationships. **(3) Bridging Local Constraints and Global Insights**: Current approaches primarily focus on global-level site selection optimization, yet lack systematic mechanisms to incorporate detailed local-level constraints during the optimization process. Consequently, practitioners can only rely on global results and must individually validate the feasibility of each candidate site, significantly reducing efficiency and scalability.

Visual analytics (VA) has been widely applied to facility location problems, including billboard placement [6], rental housing selection [7], and fire station siting [8], and has emerged as a critical tool for addressing such multi-criteria spatial decision challenges. However, its potential to optimize vertiport site selection remains largely unexplored. **In contrast to previous studies, vertiport site selection requires a comprehensive evaluation of three-dimensional spatial constraints and a systematic approach to integrating local feasibility constraints into global-scale planning objectives**. To address the aforementioned challenges, we work closely with three domain experts in the UAM area to develop visual analytics techniques for vertiport site selection. Following a user-centered design process, we derive a set of multi-level analytical and visualization tasks based on the interviews and discussions with our experts. As a result, we develop *VISTA*, a visual analytics framework that integrates multi-criteria decision-making and multi-view interactive visualization for vertiport site selection. *VISTA* enhances traditional decision-making models by incorporating 3D spatial

H. Zeng, W. Huang, X. Zhu, Y. Peng, W. Shi, and S. Zhou are with Sun Yat-sen University.

Q. Li is with the School of Information Science and Technology, ShanghaiTech University.

constraints, such as airspace regulations, terrain variations, and building heights, ensuring that selected sites account for both regulatory and physical limitations in low-altitude urban environments. To facilitate user-involved exploration, *VISTA* provides coordinated 2D and 3D views that encode demand, accessibility, cost, and safety constraints through radial glyphs, color-coded scales, and 3D modeling. Users can navigate across three hierarchical levels—global overview, cluster-level summaries, and candidate-level detailed comparisons—to inspect these indicators at the appropriate scale. Meanwhile, they can interactively adjust weights and observe real-time ranking changes across linked views, with a ranking learning mechanism applying refined preferences globally and enabling users to extrapolate localized decisions into broader planning insights. By offering a data-driven and user-centered approach, *VISTA* enhances transparency and efficiency in the eVTOL site selection process. The primary contributions of this work are as follows:

- We characterize the issues in the context of vertiport site selection process through an observational study and a thorough discussion of the design requirements with domain experts.
- We propose *VISTA*, the first visual analytics framework for eVTOL vertiport site selection. It couples multi-scale spatial exploration with interactive multi-criteria ranking, informed by a systematic exploration of visual encodings and expert feedback.
- We validated *VISTA*'s practical applicability and effectiveness through real-world case studies, expert interviews, and a user study, confirming its value for visual analytics–driven urban air mobility planning.

II. Related Work

This section presents two relevant topics, UAM planning and vertiport site selection, visual analytics for site planning.

A. UAM Planning and Vertiport Site Selection

Site selection for electric vertical take-off and landing (eVTOL) vertiports is a critical component of the urban air mobility (UAM) ecosystem. Early studies established foundational principles: compliance with airspace restrictions, meteorological conditions, and electromagnetic environments [9], [10], such as avoiding no-fly zones and coordinating with military activity areas. Traffic flow, population density, geographic location, and connectivity to existing transport infrastructure were also emphasized as essential factors for ensuring convenient and efficient aerial travel.

As research has progressed, Multi-Criteria Decision Making (MCDM) methods have emerged as the mainstream solution in this field due to their capability to systematically integrate multi-dimensional influencing factors, typically combined with Geographic Information Systems (GIS) for two-dimensional spatial analysis. MCDM methods have established a systematic application framework in facility location, particularly suitable for complex location scenarios requiring the consideration of multi-dimensional factors [11]. Current research primarily presents three development directions:

In terms of the indicator system, early studies established foundational principles, including traffic flow, population density, geographical location, environmental impact, and connectivity with existing transportation infrastructure [12], [13]. Rothfeld et al. [14] further integrated multi-source spatial data such as population, employment, POI, and transportation nodes on GIS platforms to construct more comprehensive evaluation frameworks. Additionally, there are indicator designs for specific application scenarios, such as vertiport networks supporting airports [15]–[18] and networks based on package delivery [19], [20].

In terms of model construction, Sheth's team [21] developed a composite suitability index that comprehensively considers factors such as location, noise, residential areas, and demand. These two-dimensional approaches typically integrate population density, proximity to transportation hubs, and land use to maximize economic benefit and coverage while minimizing travel costs [16], such as reducing commuting time by establishing vertiports [22]–[25].

In terms of optimization objectives, Rahman et al. [26] proposed a composite optimization model that not only minimizes network distance to bus stations but also uses population and income characteristics as demand adjustment factors, ultimately determining the optimal vertiport layout for 11 supervisory districts in San Francisco. Shin et al. [27] considered various factors in the hub location of air taxi networks, including traffic congestion, collision risks, system costs, and airspace design, to optimize the design of air taxi networks. Barsotti et al. [28] also emphasized the sustainability and social impact of cities, ensuring that the urban environment and residents' quality of life are not negatively affected. Lim et al. [29] began incorporating multiple criteria such as air travel demand, traffic load, construction costs, and environmental impact for optimization.

However, traditional MCDM methods face two key challenges in Urban Air Mobility (UAM) scenarios: First, the static weighting mechanism is difficult to adapt to the heterogeneous needs of different urban functional areas. Second, there is a knowledge transfer barrier between local optimization experience and global network planning. These issues are particularly prominent in the vertiport site selection in the airspace environment of megacities. Ranking learning models, due to their dynamic optimization characteristics, provide new ideas for solving these problems [30]. Methods such as RankSVM and LambdaMART provided by the RankLib algorithm library have been successfully applied in logistics, transportation network optimization, and other fields [31], [32]. Relevant studies have proven their effectiveness in balancing cost, accessibility, and environmental impact [33], and they have also shown good adaptability in special scenarios such as hazardous materials facility location [34].

To address these challenges, this paper presents a ranking learning-based approach. It features two key technical components: (1) an interactive, drag-and-drop ranking module for generating region-specific weight schemes in real time, and (2) a ranking learning model with feature propagation to enable the intelligent transfer of locally optimized weights.

B. Visual Analytics for Site Planning

Visual analytics has been widely applied to site planning problems. Previous research has established design patterns for composite visualizations, emphasizing the importance of multiple and coordinated views in information visualization [35] [36]. We structure the following review along three dimensions central to our work: multi-view coordination and scale-switching, visual encodings for spatial decision-making, and 3D urban environment analytics.

Multi-view coordination and scale-switching. Effective site planning often requires exploring spatial phenomena across multiple scales, from city-wide distributions down to individual candidate locations. Previous systems have demonstrated how linked, multi-view designs support this progressive exploration. For instance, Liu et al. [6] studied billboard placement with coordinated views that simultaneously show city-level traffic flows and street-level vehicle speeds. Weng et al. [7] supported rental housing selection by linking accessibility metrics with spatial views, enabling users to compare location alternatives across different criteria. Chen et al. [8] researched fire station location using coordinated views to analyze fire-related factors and simulate historical demand at multiple spatial granularities. Zhang et al. [37] optimized electric vehicle charging station placement by coupling traffic network views with power grid visualizations. Zhang et al. [38] designed SpoVis for sports facility site selection, explicitly supporting both macro-level distribution analysis and micro-level site evaluation within a digital twin environment.

Visual encodings for spatial decision-making. Spatial site selection inherently involves balancing multiple, often conflicting criteria, and the choice of visual encoding significantly affects a planner's ability to perceive and resolve such trade-offs. Yu et al. [39] proposed an interactive visual analytic system called AdvMOB, which integrates personal information, trajectory data, and urban architectural insights to evaluate and scrutinize digital outdoor billboard exposure within urban landscapes and to clearly delineate the genuine reach of each advertisement, thereby addressing the issues in current ad placement models that overlook ad effectiveness and oversimplify advertising influence. Weng et al. [40] proposed a spatial ranking visualization technique called SRVis, which addresses three major challenges in large-scale spatial multi-criteria decision-making—context integration, scalability of ranking representations, and analysis of context-integrated rankings—through matrix-based visualizations, stacked bar charts, and a two-phase optimization framework. In the energy domain, Pammi et al. [41] proposed a visual analytics framework for renewable energy resource planning, supporting the exploration of spatiotemporal patterns in solar and wind data alongside equipment site assessment. Additionally, important study on store location [42] and ambulance station location [43] have incorporated spatial data analytics. Radial visual encodings, which prior empirical work has shown to facilitate pattern recognition in small-multiple comparisons and multi-criteria evaluation tasks [44] [45], are adopted in our candidate assessment glyphs for these reasons.

3D urban environment analytics. Recent visual analytics research has begun integrating three-dimensional spatial contexts to better reflect the complexity of urban environments. Zou et al. [46] integrated geospatial big data with mobile signaling data and further employed 3D reconstruction techniques to enable immersive commercial site selection analysis, demonstrating the value of 3D representation for understanding spatial relationships that are invisible in 2D views. Ferreira et al. [47] focus on 3D urban environment analytics, proposing a 3D framework integrating multi-source data to support data-driven urban development decisions, consistent with Urbane's core purpose. Mota et al. [48] explore the effectiveness of diverse visual strategies for 3D spatiotemporal urban data visualization and offer targeted design guidelines.

While visual analytics has demonstrated remarkable success in traditional facility siting applications, its implementation in vertiport location planning faces several unique challenges. Urban air mobility scenarios present three fundamental distinctions: Firstly, in terms of dimensional complexity, vertiport site selection requires coordinating air corridors, demand distribution, and urban obstacles within a comprehensive 3D evaluation framework—a level of 3D integration rarely supported in current VA site selection tools. Secondly, regarding safety specifications, aviation-specific parameters such as vertical approach buffers and wake turbulence zones must be incorporated, demanding specialized visual representations to be properly assessed by human planners. Thirdly, concerning system integration, reconciling localized constraints with network-wide planning objectives calls for interactive mechanisms that not only visualize local trade-offs but also propagate user decisions across scales.

To address these challenges, we propose *VISTA*. Its design combines multi-scale spatial views (global/cluster/candidate) for progressive exploration of 3D-constrained sites, radial glyphs and bubble sets for encoding multi-criteria trade-offs, and a ranking learning mechanism that transfers localized weight preferences across the city. The system integrates building morphology, airspace restrictions, and demand characteristics—using data from over 2,000 high-rises in Shenzhen, aviation controls, and millions of trip records—into a unified 3D platform for interactive exploration and refinement.

III. Observational Study

A. Domain Experts

Vertiport site selection involves domain experts from diverse backgrounds—such as government planners and researchers—each bringing distinct priorities and constraints to the process. To better understand these varied perspectives and inform the design of our visual analytics system, we conducted 1-hour one-on-one interviews with three experts (E1–E3), whose insights helped shape the functional requirements of our system.

- E1 (male, 38) – official at the Municipal Development and Reform Commission, in charge of eVTOL infrastructure projects;
- E2 (male, 41) – associate professor with 15 years of research in aviation safety management, airspace utilization, and vertiport site selection;

• E3 (male, 37) – associate professor at a local university, with 12 years of experience in urban transportation and aviation;

B. Interview Content

During the interviews, participants were asked to describe their site selection process. According to the experts' statements, the site selection workflow is a systematic process. The process begins with determining the functional positioning of the vertiport and the main aviation business indicators, followed by a detailed site analysis that includes assessments of geographical location, site conditions, airspace conditions, air domain conditions, meteorological conditions, environmental conditions, energy supply, transportation conditions, public utilities, land use, relocation and renovation situations, as well as the sources of construction materials. Each analysis step aims to ensure that the selected site can meet various requirements such as safety, operations, and environmental considerations, and supports decision-making by collecting and analyzing relevant data. Ultimately, all analysis results are compiled to determine the most suitable location for the vertiport. Participants were also asked to describe the key factors they consider when selecting vertiport sites, as well as other relevant aspects of the siting process. E1, for example, emphasized that safety is the top priority: "From an urban-development perspective, our foremost task is to ensure safety before pursuing any benefits. The success of a project hinges on delivering safe, efficient infrastructure within budget." E2 stated, "My focus is on technical feasibility. A site must have stable geology, unobstructed airspace, and good infrastructure access; any location with a low safety margin is simply not viable." Meanwhile, E3 underscored the importance of incorporating social and environmental impacts into the decision-making process, stressing that the siting procedure should fully account for effects on surrounding communities and strive to balance multiple competing factors.

Based on the above interviews, we summarize the key findings into the following three aspects.

Latent passenger demand The core customer group for eVTOL is high-end business travelers, corporate travelers, and time-sensitive users. At present, large-scale operational data are lacking, so taxi demand is commonly used as a proxy: areas with high taxi-ride frequency are regarded as regions with strong eVTOL demand. E3 pointed out, "Air-taxi users place extremely high demands on efficiency; vertiport site selection must precisely match their travel needs."

Key siting factors In addition to demand, it is necessary to simultaneously weigh safety, accessibility, cost, and environmental impact. Safety: current regulations have yet to specify urban low-altitude safety buffers and air corridors, and quantitative standards are lacking. Accessibility: vertiports must connect to airports, subways, and business districts, yet high-demand areas are often space-constrained. Economics: high initial investment and uncertain returns cause private capital to remain on the sidelines. Environmental impact: vertiports need to consider the noise impact on surrounding locations. Decision framework: there is no unified multi-criteria weighting system, evaluation standards vary by locality, and the process is subjective and inefficient.

eVTOL siting workflow Experts typically adopt a three-stage process: "demand clustering → 3-D safety screening → site planning." 1) Demand clustering: use data on traffic flow and population distribution to identify hotspots; E1 stated, "Analyzing congested areas and densely populated zones lets us pinpoint high-demand locations." 2) 3-D safety screening: traditional methods consider only two-dimensional geographic constraints and ignore vertical factors such as building heights and aerial obstacles; E3 cautioned, "Conventional practice only looks at geographic location and ignores 3-D airspace safety, which entails risks." 3) Site planning: standardized assessment tools are lacking, so local constraints must be checked manually one by one, resulting in a fragmented, labor-intensive workflow. An integrated, data-driven tool is needed.

Although the experts did not explicitly invoke visualization, their accounts revealed a clear need for interactive, visual tools to address the spatial complexity and multi-criteria trade-offs inherent in vertiport siting.

C. Requirement Analysis

Following the design study methodology [49], we structured our work across its nine phases. The Learn phase consisted of a literature review (Section II); Winnow and Cast narrowed the scope to interactive visual analytics for multi-criteria decision-making by UAM planners in Shenzhen, informed by the expert findings in Sections III-A and III-B; Discover distilled the following requirements (Section III-C); Design and Implement produced the system architecture (Sections IV–VI); Deploy involved the case studies and expert evaluation (Section VII); Reflect addressed the findings and limitations (Section VIII); and Write encompassed the design rationale articulated throughout this paper and the future directions summarized in Section IX. Based on the expert interviews and iterative discussions, we distilled the following visualization-centered requirements to guide the system design:

R.1 Explore multi-source spatial data across scales. Users need to examine and correlate diverse spatial datasets—including traffic demand patterns, population distribution, 3D building morphology, airspace regulations, and Points of Interest—at city, cluster, and candidate levels. The system should provide coordinated views that allow users to seamlessly navigate across these spatial scales while maintaining contextual awareness of all data layers.

R.2 Inspect 3D airspace constraints for safety verification. Users need to visually assess whether a candidate site satisfies flight-operation safety requirements in three dimensions—specifically, whether building heights, terrain variations, and no-fly zones obstruct approach and departure paths. The system should render vertical obstacles in relation to takeoff/landing trajectories and safety buffers, enabling users to quickly identify sites with insufficient airspace clearance.

R.3 Compare multi-criteria trade-offs among candidate sites. Users need to simultaneously evaluate competing criteria—such as demand, accessibility, cost, and noise sensitivity—across multiple candidate sites while understanding the

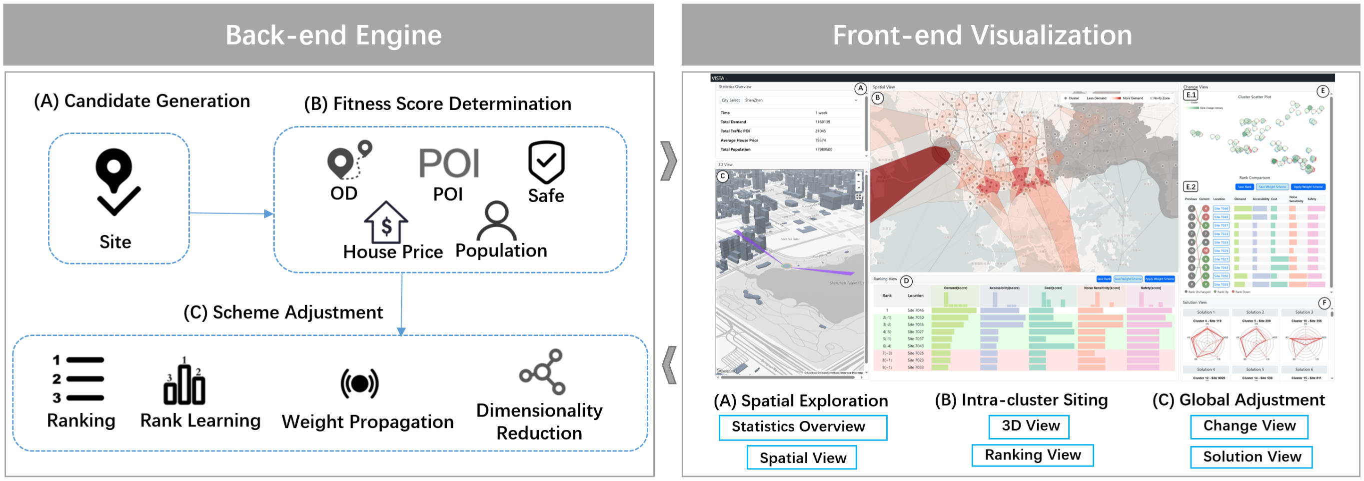

Fig. 1. The system architecture consists of two parts: a back-end engine and a front-end visualization. The back-end engine includes three modules: Candidate Generation, Fitness Score Determination, and Scheme Adjustment. The front-end visualization provides six designed views, categorized into Spatial Exploration, Intra-cluster Siting, and Global Adjustment, to support efficient analysis.

3D spatial context of each location. The system should support interactive criteria weighting and provide visual encodings that reveal how changes in one factor propagate through the overall ranking, helping users reason about trade-offs in real time.

R.4 Iteratively refine rankings to accommodate local constraints. Users need to adjust the relative importance of evaluation criteria within specific local areas, because optimal weight configurations vary across urban functional zones. The system should allow users to interactively modify weights, observe the resulting ranking changes across all linked views, and capture the refined preference model so that localized decisions inform city-wide planning.

R.5 Generate and compare alternative siting solutions. Users need to evaluate multiple candidate configuration scenarios side by side to understand how different parameter settings affect the final set of recommended sites. The system should enable users to save, load, and compare different weight schemes and their corresponding ranking outcomes, facilitating comprehensive assessment before final selection.

IV. Approach Overview

We introduce *VISTA*, an interactive visual analytics system that supports the iterative selection of vertiport sites across multiple spatial scales. The system architecture (Figure 1) consists of two main components: a back-end engine and a front-end visualization.

The back-end engine is responsible for data processing and optimization. It includes three modules—Candidate Generation, Fitness Score Determination, and Scheme Adjustment—that together screen candidate sites, compute multi-criteria fitness scores, and apply a ranking learning algorithm to propagate locally adjusted weight preferences across the entire city. The technical details of these modules are provided in Section V.

The front-end visualization is the primary workspace for analysis and decision-making. It comprises six coordinated views organized around a progressive analysis workflow. The Statistics Overview provides a summary of urban demand, housing prices, and population characteristics. The Spatial View supports multi-scale exploration across three hierarchical perspectives—global level, cluster level, and candidate level—encoding demand intensity, accessibility, cost, and safety constraints through radial glyphs, bubble sets, and color-coded scales (**R.1**, **R.3**). The 3D View renders building models and aviation safety zones, enabling users to assess the feasibility and safety of flight paths (**R.2**). The Ranking View and Change View together support interactive weight adjustment: users can drag to reorder candidate sites, save refined weight schemes, and observe ranking changes reflected in real time across linked views (**R.4**). The Solution View allows users to record, display, and manage site selection results, using radar charts to visualize key metrics across candidate sites (**R.5**). All views are linked through multi-view synchronization, enabling a detailed and scalable exploration of site selection factors. The detailed visual design and interaction mechanisms of each view are described in Section VI.

V. Back-end Engine

A. Data Description

Following multiple iterative rounds of validation and requirement refinement with three domain experts, this study takes Shenzhen as the research area and collects five key types of data: 1) **OD Data** (Origin–Destination Data): ride-hailing and taxi service records from Shenzhen (February 4–11, 2024, 1,160,139 records), capturing travel patterns, pickup/drop-off locations, and timestamps. 2) **POI Data** (Points of Interest): detailed information on transportation hubs in Shenzhen. 3) **3D City Building Data**: building shapefiles with heights, facade structures, and spatial layouts for eVTOL safety assessment. 4) **Housing Price Data**: real estate pricing across districts and property types, used as a reference for construction cost estimation. 5) **Street Population Data**: resident population size, density, and demographic structure at the street level.

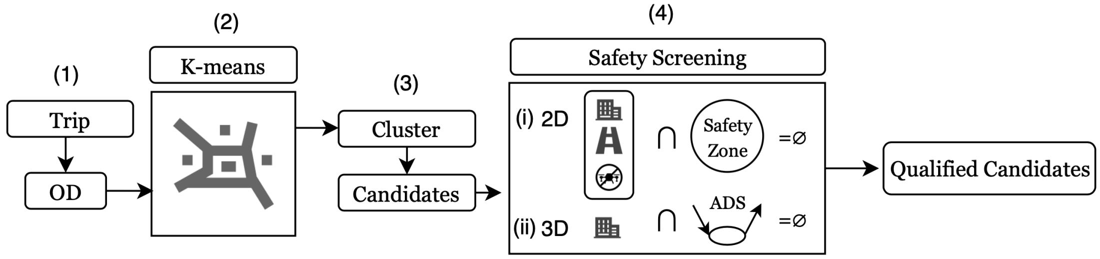

Fig. 2. Workflow of Candidate Generation: (1) Trip data processing extracts origin-destination (OD) pairs from ride-hailing records. (2) OD points are clustered using K-means (k=200) to identify demand hotspots. (3) Within 1000 m radius zones centered on the cluster centroids, the system generates random candidate points. (4) Candidates undergo a two-phase safety screening process: (i) 2D spatial filtering and (ii) 3D airspace verification. Operational zones are defined based on UAV specifications (D = 17 m wingspan): TLOF (1.0D), FATO (1.5D), and a safety zone (1.75D) with a 15% approach slope.

B. Candidate Generation

Candidate Generation consists of three steps: demand clustering, generating random candidate points, and 2D/3D safety screening. Each is described in turn below.

Demand clustering. In the process of generating the vertiport site selection plan, data preprocessing is a key step to ensure the accuracy and effectiveness of the site selection model. Using origin–destination (OD) data, we take the start and end points of ride-hailing orders as demand points. To maximize coverage, these points are clustered, with each cluster serving as a decision unit. We apply the K-means algorithm to cluster the demand points due to its speed and scalability with large datasets. After comprehensively evaluating intra-cluster compactness and inter-cluster separation using the Davies–Bouldin Score, we set the number of clusters to 200. This ensures full demand coverage while providing Shenzhen with a sufficient pool of candidate sites for its planned vertiports. The resulting 200 clusters provide the demand distribution basis for the subsequent site-selection model. We screen these clusters against no-fly zones, reducing the number of valid clusters from 200 to 140. In subsequent computations, each of these 140 valid clusters is treated as a local zone, and exactly one vertiport location is selected within each zone.

Generating random candidate points. Expert E2 noted that 1 km is commonly used as a rule-of-thumb service radius in urban cores. Rather than adopting this value directly, we treat it as a tunable parameter and employ PPO (Proximal Policy Optimization) [50] to automatically determine a suitable radius and candidate count per cluster that balance spatial coverage with computational efficiency. The search ranges from 500 m to 2500 m for radius and 50 to 400 for candidates per cluster. The resulting configuration—1000 m radius and 100 candidates per cluster—yields approximately 14,000 candidates city-wide. Candidate points are randomly sampled within each cluster's convex hull to ensure geographic relevance before subsequent safety screening. The scale of each candidate point is defined by aviation operational requirements. We assume a maximum wingspan (D) of 17 meters. Each candidate point consists of three nested zones: the Touchdown and Lift-Off Area (TLOF, radius 1.0 D), the Final Approach and Take-Off Area (FATO, radius 1.5 D), and the Safety Area (radius 1.75 D). The approach and take-off surfaces have a spread rate of 15% and extend vertically to 152 meters above the FATO, where their width reaches 10.0 D [51], [52].

2D and 3D safety screening. Each candidate point undergoes two-dimensional and three-dimensional safety screening. In the two-dimensional space, points that intersect with the safety zone, building buffer zones, road network buffer zones, or no-fly zones are excluded. In the three-dimensional space, the candidate point must meet the requirement that the approach-departure surface (ADS) do not intersect with buildings, ensuring the safe operation of the vertiport.

C. Fitness Score Determination

Using preprocessed data, we construct a site selection model to determine fitness scores: within each cluster, we calculate the comprehensive fitness score for each candidate location based on five integrated indicators—demand, accessibility, safety, cost, and noise sensitivity. All five indicators are normalized. Among them, the Demand Score (DS) reflects the ability of the candidate site to cover demands within the cluster; it depends on the number of demand points within each cluster and the average distance from each cluster to that candidate location. The Accessibility Score (AS) is related to the traffic scale score (facility scale) of POIs in the local area and the distance between the candidate point and POIs, used to evaluate connectivity with existing transportation networks and facility scale. The Safety Score (SS) sets a threshold based on the number of unobstructed runways (minimum 2) to ensure operational safety. The Cost Score (CS) is determined by the housing prices of properties nearest to the candidate point, reflecting the economic feasibility of the site. The Noise Sensitivity Score (NSS) quantifies environmental impact by combining population density with the proportion of elderly residents. Specific calculation formulas are detailed in the supplementary materials. After normalizing the five indicators, the comprehensive fitness score (FS) is computed as follows:

$$\begin{aligned} FS = \omega_1 \times DS_{\text{norm}} + \omega_2 \times AS_{\text{norm}} + \omega_3 \times SS_{\text{norm}} \\ + \omega_4 \times (1 - CS_{\text{norm}}) + \omega_5 \times (1 - NSS_{\text{norm}}), \end{aligned} \tag{1}$$

where ω_i denotes the weight coefficient, with $\sum_i \omega_i = 1$, which users can adjust according to practical needs to meet diverse optimization objectives. Initially, we set each weight coefficient ω_i to be equal. Specifically, each weight coefficient ω_i is set to $\frac{1}{5}$.

This article has been accepted for publication in IEEE Transactions on Visualization and Computer Graphics. This is the author's version which has not been fully edited and content may change prior to final publication. Citation information: DOI 10.1109/TVCG.2026.3712668

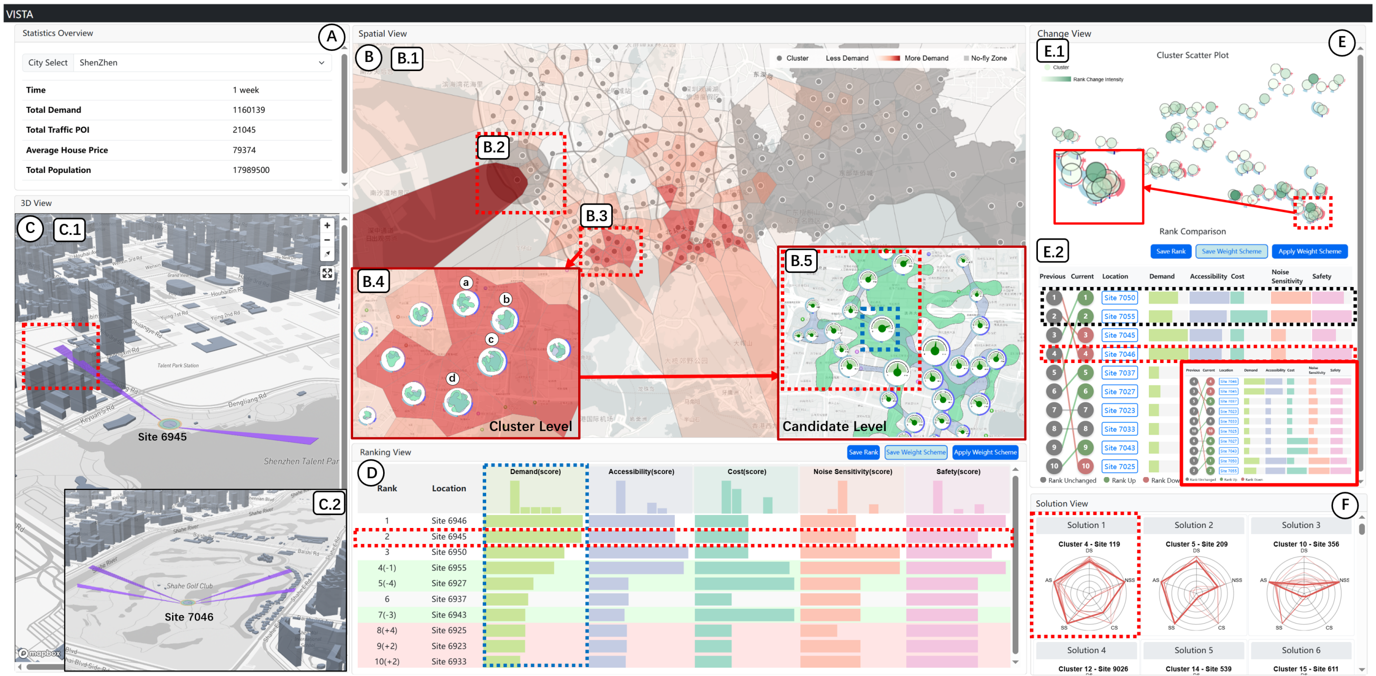

Fig. 3. The system overview of *VISTA*. (A) The Statistics Overview displays aggregated urban metrics, including total demand, total traffic POI, average house price, and total population. (B) The Spatial View presents multi-scale geovisualization of demand hotspots and supports multi-criteria comparison across global, cluster, and candidate levels. (C) The 3D View constructs building models and aviation safety zones to verify spatial safety of landing/takeoff zones. (D) The Ranking View provides interactive reordering and weight adjustment with ranking learning. (E) The Change View reveals cluster similarities and ranking dynamics through t-SNE projection. (F) The Solution View compares alternative siting configurations via radar charts.

D. *Scheme Adjustment*

The ranking of candidate points is obtained by sorting them in descending order of fitness scores. To achieve city-wide weight consistency, we adopt LambdaMART [53], a Learning-to-Rank algorithm that combines Gradient Boosting Decision Trees with the LambdaRank framework. LambdaMART learns optimized weights from the ranking adjustments made by users in the front-end visualization, and these weights are then propagated across all clusters to maintain global consistency. This propagation is essential because uniform UAM regulations and safety standards mean that large inter-cluster weight disparities could introduce compliance risks, and passengers expect comparable service quality regardless of district.

VI. Front-end Visualization

VISTA consists of six main components (Figure 3). This section introduces the visual design of each view, explaining how they address the requirements identified in Section III-C.

A. *Statistics Overview*

The Statistics Overview (Figure 3 (A)) provides a summary of urban demand, Points of Interest (POI), housing prices, population density, and the proportion of elderly people. At the top of this view, a control panel allows users to load datasets from different cities. A table displays key statistical information, including time, total demand, total POI, average housing prices, population density, and the proportion of elderly people (**R.1**).

B. *Spatial View*

The Spatial View (Figure 3 (B)) serves as a comprehensive spatial analysis tool for site selection planning, integrating multi-source data such as demand, no-fly zone distribution, transportation-related POI, population density, and housing prices (**R.1**, **R.3**). To accommodate different levels of analysis, this view is structured into three hierarchical perspectives: global level, cluster level, and candidate level, enabling a detailed and scalable exploration of site selection factors.

At the global level (Figure 3(B.1)), we treat the origin–destination pairs extracted from ride-hailing orders as demand points, partition the space with a Voronoi tessellation, and cluster these points with a density-based algorithm [54]. The color of each Voronoi cell encodes the demand intensity of its corresponding cluster: after applying a log-transform to the total order volume within each cluster, we divide the distribution into five demand levels using the 25th, 50th, 75th, and 90th percentiles as thresholds and map them to a red gradient that darkens with increasing intensity; transparency is progressively raised so that high-demand zones remain visually prominent above the basemap. To assist users in rapidly recognizing both demand patterns and restricted areas, we overlay the global view with no-fly zones rendered as a 10 % opaque dark grey mask.

When the user zooms in on the map to a specific level, it transitions to the cluster level (Figure 3 (B.4)). At this stage, detailed information for each cluster is displayed (Figure 4 (a)): The radius of the circle reflects the number of demand points within the cluster, while the purple box plot to the right of the circle shows the distribution of housing prices.

This article has been accepted for publication in IEEE Transactions on Visualization and Computer Graphics. This is the author's version which has not been fully edited and content may change prior to final publication. Citation information: DOI 10.1109/TVCG.2026.3712668

The light blue and dark blue arcs on the left side of the circle represent the population density of the corresponding streets, with the dark blue portion indicating the proportion of the elderly population. Additionally, the central Bubble Set visually represents the relative geographical distribution of traffic POIs and candidate points within the cluster. Traffic POIs are connected by blue Bubble Sets, while candidate points are connected by green Bubble Sets, making it easier for users to differentiate between the two types of points.

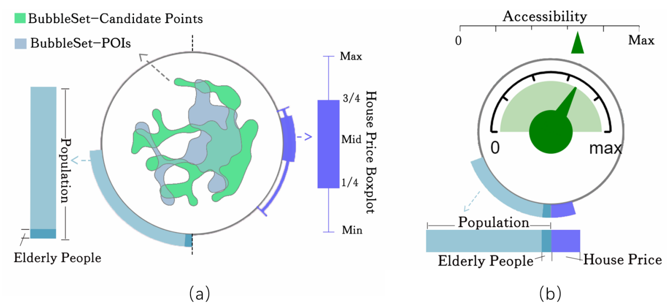

Fig. 4. Glyph design for cluster and candidate point analysis. (a) Cluster Level: This glyph shows the detailed information of clusters, including the number of demand points, housing price distribution, population distribution, and the geographical distribution of transportation POIs and candidate points. (b) Candidate Level: This glyph displays the detailed information of candidate points within each cluster, including demand scores, cost scores, population distribution, and accessibility scores.

Furthermore, upon clicking on a cluster, the user transitions to the candidate level (Figure 3 (B.5)), where detailed information for each candidate point is displayed (Figure 4 (b))(**R.3**)). Specifically, this includes: the demand score represented by the radius of the circle, the accessibility score indicated by the pointer on the dashboard of the inner circle, the population density shown in the light blue section of the left arc of the outer circle, the proportion of the elderly population indicated by the dark blue section of the left arc of the outer circle, and the cost score displayed in the purple right arc of the outer circle. Meanwhile, the Bubble Sets in Figure 4(a) are one-to-one mapped onto the map: the distance between each candidate site and the green transit-POI Bubble Set instantly reflects its accessibility, allowing users to evaluate a station's locational advantage in seconds without changing views.

At the same time, this view offers rich interactive features, such as sending information to the 3D View when the user clicks on a cluster, enabling multi-view linkage, and enhancing the user experience with map zooming and information prompt boxes.

Justification: Figure 5 illustrates the alternative glyph designs we considered while designing the Spatial View.

In the glyph design process for the cluster level, initially, we attempted to present the detailed population and housing-price information for each cluster using bar charts and violin plots (Figure 5 (a)). However, this approach suffered from low spatial efficiency: bars and violins require extra padding, and comparative performance was poor—the difference in median housing prices between two clusters was less discernible than with the circular glyph's boxplot. Additionally, the encoding channels were redundant; violin plots use width for density and length for price quantiles, while bar height encodes population density, resulting in a dual-length encoding. We therefore switched to a circular glyph that maps all statistics onto radial channels (radius, angle, arc length), eliminating axial conflicts (Figure 4 (a)).

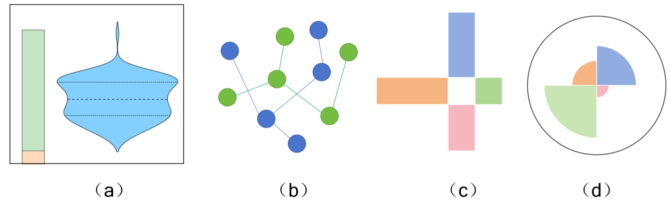

Fig. 5. Alternative designs. In the initial site-glyph designs, we used bar charts to represent population and violin plots to show housing prices (a), and connected POIs and sites with straight lines (b). We also used bar charts (c) or pie charts (d) to display the four metrics of the sites.

In the glyph design process for the candidate level, initially, we attempted to link transit POIs and candidate sites with straight lines (Figure 5 (b)) to indicate their spatial overlap. After consulting visualization experts, however, we identified two major drawbacks: it is impossible to determine how multiple circles should be connected, and the degree of overlap cannot be quantified, making direct comparison difficult. Following expert recommendations, we adopted Bubble Sets instead [55]: transit POIs are grouped by a blue bubbleset, while candidate sites are grouped by a green bubbleset. The contour area of each Bubble Set and the size of their overlap immediately convey the density and coincidence of the two point sets—the larger the contour, the more POIs or sites it contains; the higher the overlap, the closer the POIs are to the sites and the more transit-accessible the area.

Initially, we proposed two glyph encodings for the site data as shown in Figure 5(c, d). Referring to the paper by Li et al. [56], Figure 5(c) encodes the four scores (demand, accessibility, population, housing price) as four separate, differently-colored bars. Figure 5(d) encodes the same four scores as four differently-colored pie segments. However, domain experts pointed out that both designs force users to perform a "graph-to-value" decoding step before they can compare sites, significantly increasing cognitive load. Moreover, the metrics are laid out flat within each glyph—no clear priority—so users cannot immediately grasp which factor is most important, hampering decision speed. Therefore, we redesigned the glyph as shown in Figure 4(b): the circle's radius directly encodes demand intensity, and a gauge needle encodes transit accessibility, creating the visual focal point. Housing prices and population distributions are relegated to adjacent bar and box plots, their visual weight deliberately reduced, because within the cluster, the differences in these two metrics between different candidates are small.

C. 3D View

The 3D View provides a detailed spatial analysis of candidate points in Shenzhen for eVTOL station site selection (**R.2**). It consists of two main components: building modeling and 3D visualization of candidate points (Figure 3 (C)).

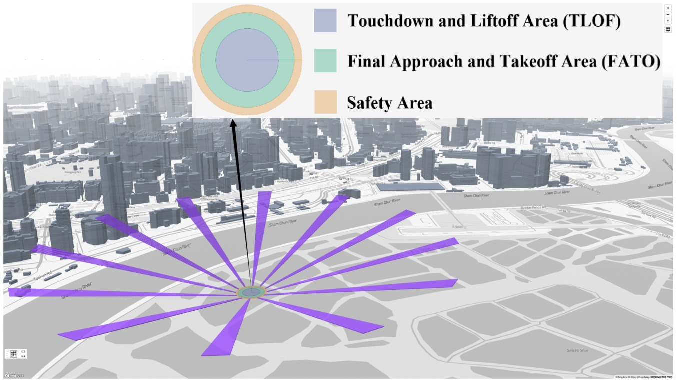

Fig. 6. Functional zoning with color-coded areas: TLOF (blue, R = 17 m), FATO (green, R = 25.5 m), Safety Area (yellow, R = 29.75 m), and the 22.5° inclined aerial runway (purple, Alt = 152 m).

Using Building Information Modeling (BIM) and Mapbox GL, buildings are modeled with fill extrusion layers, rendering details only at zoom level $\geq$ 12 to reduce computational load [48]. Building heights are mapped from GeoJSON data, with semi-transparent fill (opacity: 0.8) to highlight structures while maintaining background visibility for contextual analysis.

Candidate points are displayed with distinct functional zones (Figure 6): Touchdown and Liftoff Area (blue, radius 17 m), Final Approach and Takeoff Area (green, radius 25.5 m), and Safety Area (yellow, radius 29.75 m). Additionally, aerial runway (purple, 22.5° incline, 152 m altitude) is modeled to assess flight path feasibility and safety. Referring to the paper by Qu et al. [57], we allow users to rotate the viewpoint to see which runways are obscured, thereby assessing the feasibility and safety of flight paths.

D. Ranking View

The Ranking View (Figure 3 (D)) adopts the stacked bar chart encoding from LineUp [58] to help users optimize candidate site rankings through interactive adjustments, supporting eVTOL site selection decisions (**R.4**). It displays the top ten ranked candidate points filtered via 3D safety screening, with each row showing the ranking, site ID, and five key indicators (demand, accessibility, cost, noise sensitivity and safety) as bar charts (**R.3**). Users can click a row to view detailed values, with synchronized updates in the Spatial View and 3D View, ensuring a comprehensive analysis. Unlike general-purpose multi-view coordination frameworks such as TPFlow [59], which targets top-down progressive partitioning of spatio-temporal data, our coordination mechanism is specifically designed for real-time ranking adjustment and coupled 2D/3D navigation in the constrained domain of vertiport siting.

Below the column headers, indicator distribution maps provide an overview of value distributions. Users can manually adjust rankings by dragging rows—green indicates an improved rank, red a decline, with intensity reflecting the magnitude of change (**R.4**). This color-coded system makes ranking modifications intuitive.

Once satisfied with the adjustments, users can click the "Save Weight Scheme" button, enabling the system to learn new ranking preferences and update the weights accordingly. When users click the "Apply Weight Scheme" button, the system applies the weight scheme globally, updates the rankings across all candidate sites, and reflects the changes in the Change View. The system continuously refines the rankings through automatic learning to ensure real-time feedback.

By integrating interactive ranking adjustments, weight learning, and multi-view synchronization, the Ranking View provides a flexible, data-driven approach to refining site selection decisions.

E. Change View

The Change View (Figure 3 (E)) visualizes cluster similarity and ranking changes, providing insights for optimizing site selection decisions (**R.4**). By applying t-SNE dimensionality reduction [60] to the multidimensional information of clusters, the system projects high-dimensional data onto a two-dimensional plane. The scatter plot within illustrates the distribution of clusters, with closer distances between scatter points indicating higher similarity. The color depth of each scatter point represents the extent of ranking changes within a cluster, with darker colors signifying greater shifts. When the mouse hovers over a point, the detailed glyph of that cluster is displayed. The embedded visual elements, consistent with the design in (Figure 4 (a)), intuitively show the distribution of housing prices, population density, and the proportion of the elderly population, helping users quickly grasp key spatial attributes.

The ranking comparison table presents changes before and after adjustment, where green dots indicate rank increases and red dots indicate decreases. The "Previous" column shows the ranking under the previous weight scheme, while the "Current" column shows the ranking under the current weight scheme. The lines connecting the two columns indicate how the ranking of the same site has shifted. Users can explore detailed indicator values through an interactive bar chart or click on a candidate site to locate it in the Spatial View and 3D View. Users can further refine the ranking by dragging and dropping candidates within the table into a custom order. This manual adjustment does not alter the underlying weight scheme; it directly overrides the displayed ranking, and clicking 'Save Rank' persists the new order to the backend.

By combining automated analysis with user-driven adjustments, the Change View ensures flexibility and transparency in site selection. Its real-time multi-view synchronization and dynamic ranking adjustments provide a powerful tool for refining decision-making, ensuring that site selection strategies remain both data-driven and adaptable to complex urban environments.

F. Solution View

The Solution View (Figure 3(F)) is designed to record, display, and manage site selection results within a specific local area, enabling users to comprehensively evaluate their final decisions (R.5). It presents the top ten candidate sites within each cluster after screening and optimization, using a radar chart to visualize key metrics, including cluster identification, site ID, and five core indicators (Demand Score (DS),

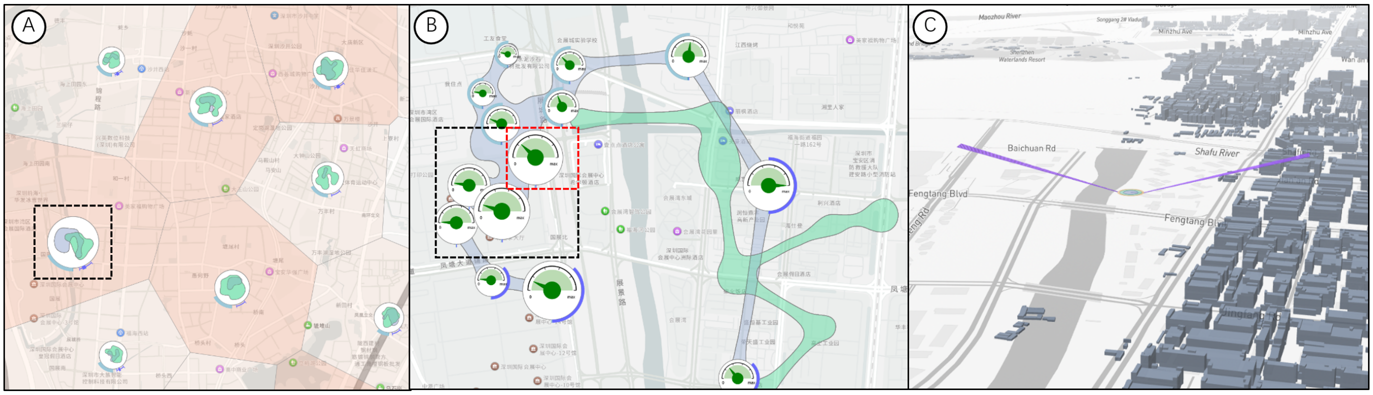

Fig. 7. E1's operations in case I. (A) E1 used glyph encodings to compare each cluster at the cluster level in the Spatial View. (B) E1 used glyph encodings to compare each candidate point at the candidate level in the Spatial View. (C) E1 examined candidate point location in the 3D View.

Accessibility Score (AS), Cost Score (CS), Noise Sensitivity Score (NSS) and Safety Score (SS)). The radar chart line for the Top 1 site is bolded. This structured layout helps users quickly assess the overall performance of each site. This radar chart design draws upon the radar chart visualization in the T-PickSeer system proposed by Gu et al. [61], which is used for analyzing taxi pick-up point selection behavior.

User interactions in the Solution View are recorded in real time and synchronized across other related views. For example, selecting a cluster in this view highlights the corresponding cluster and final site on the Spatial View, and vice versa, ensuring a seamless multi-view interactive experience.

VII. Evaluation

We perform two case studies and conduct interviews with domain experts. Section VII-A elaborates on the two representative cases executed by experts E1 and E2. The insights gathered from domain experts are consolidated in Section VII-B. Subsequently, a user study was conducted with 10 additional participants to assess the performance of *VISTA*, focusing on its in system workflow, visual design and interaction, as well as system usability; the findings of this study are elaborated in Section VII-C.

A. Case Studies

1) Case I: Multi-Criteria Decision Analysis for Site Selection in Guangming District: This case demonstrates how multi-view collaborative analysis can be leveraged to achieve optimal site selection in Guangming District and to validate the results.

E1 designated Guangming District as the target construction area. Since the government has explicitly planned to build an integrated transportation hub there, E1 focused directly on the district in the Spatial View. After zooming in and switching to the cluster level, E1 noticed that one cluster's glyph had a significantly larger radius than the others (black dashed box in Figure 7(A)), and its box plot showed low housing prices. This indicated the highest overall demand and the lowest construction costs. Consequently, E1 clicked on this cluster.

E1 analyzed each candidate point's multi-dimensional performance using glyphs in the Spatial View. At the candidate level (Figure 7(B)), E1 used glyph encodings to compare each site across multiple dimensions: population, housing price, demand score, and accessibility. The length of the purple arc on the right fell into 2 distinct levels, indicating 2 price tiers; the blue arc on the left had two levels (min and max), revealing two population tiers. Based on these cues, E1 first narrowed the candidate set to the cluster with the lowest housing prices and lowest population (black dashed box in Figure 7(B)). Within this cluster, he selected the site with the highest accessibility score (red dashed box in Figure 7(B)) to maximize residents' travel convenience. After this preliminary choice, E1 inspected the location in the 3D View (Figure 7(C)) and confirmed unobstructed flight corridors, meeting safety requirements. The final selected site closely matched the location recommended by E1, thereby validating *VISTA*'s practical utility for site selection. He noted that the visualization immediately showed where approach surfaces were blocked by buildings, saving several rounds of onsite verification.

2) Case II: Optimize Site Selection for High-Demand Areas through Multi-View Analysis: This case illustrates how multi-view collaborative analysis can be leveraged to optimize site selection for high-demand areas.

E2 identified demand-concentrated areas by selecting the target city in the Statistics Overview. E2 began by selecting Shenzhen as the target city in the Statistics Overview (Figure 3(A)). Given the constraints of a limited government budget, the primary objective was to maximize coverage of high-demand areas. In the Spatial View (Figure 3(B.1)), the heatmap revealed an area with significantly darker coloration compared to its surroundings (Figure 3(B.2)), indicating a high concentration of potential demand. However, since this area overlapped with a no-fly zone, E2 explored an alternative high-demand region (Figure 3(B.3)). E2 zoomed into the alternative region, switched to the cluster level (Figure 3(B.4)), and examined the cluster-representing glyphs for further analysis.

E2 analyzed population distribution in the Spatial View to identify higher-demand clusters. First, he narrowed the scope to the four clusters with the largest radius (Figure 3(a, b, c, d in B.4)), then selected the three clusters where the Bubble Sets of POIs and sites overlapped most (Figure 3 (b, c, d in B.4)). While comparing cluster characteristics, he noticed that one cluster's boxplot sat markedly lower overall, indicating the lowest construction cost, so he clicked on that cluster (Figure 3 (d in B.4)). After the click, the view switched to the candidate level (Figure 3 B.5). E2 noticed that the blue arcs on the left of all candidate points were identical in length, indicating that their population data were exactly the same—an outcome of their all belonging to the same census block. He also saw that the blue arcs to the right of the circles were split into only two lengths—maximum and minimum—revealing that the candidates have just two distinct housing prices. To minimize costs, he filtered the candidate set to keep only those with the shorter blue arcs (see the red dashed box in Figure 3 (B.5)). From the perspective of demand, the glyph of the centrally located site has the largest radius, indicating the highest demand intensity of the location. Meanwhile, the dashboard pointer of this glyph has reached a relatively large value, and the site is situated within the bubble set of Points of Interest (POIs). This not only shows that the site has high demand but also indicates excellent accessibility (as shown in the blue dashed box in Figure 3(B.5)). Fine-grained differences among these central sites and their safety compliance will be determined later via the 3D View (Figure 3(C)) and the Ranking View (Figure 3(D)).

E2 sorted candidates by demand score in the Ranking View and saved the weight scheme. The Ranking View (Figure 3(D)) displays the top ten sites that passed the safety screening. Prioritizing maximum demand, he first arranged the candidates in descending order of demand score (red dashed box in Figure 3(D)). Next, E2 clicked each one to verify geographical safety. He found that Site 6945 has only two aerial runways, one of which passes through a building (red dashed box in Figure 3(C.1)), so he removed it from the list (the red dashed box in Figure 3 D). E2 locked this sorting criterion with the "Save Weight Scheme" function and synchronized it across all other clusters via the "Apply Weight Scheme" button in the top-right corner of Figure 3(D).

E2 discovered anomalous ranking fluctuations in the Change View. In this view (Figure 3(E.1)), he observed a dense cluster of dark-green points (red dashed box in Figure 3(E.1)); their tight distribution suggested similar baseline conditions, a conclusion reinforced by the housing-price box plots on the right and the population bar charts on the left (red solid box in Figure 3(E.1)). The deep green of these cluster points indicates that the rankings of candidates within these clusters changed dramatically before and after E2 applied the "Save Weight Scheme", prompting E2 to investigate why. E2 clicked a point to examine detailed ranking changes (Figure 3(E.2)).

E2 re-evaluated the candidate priorities by integrating data from other indicators. The results show that the noise-sensitivity bars for the top-ranked candidates (Site 7050 and Site 7055) are long (black dashed box in Figure 3(E.2)), indicating that both sites are highly sensitive to noise (Figure 3(E.2)). Returning to the scatter plot (red dashed box in Figure 3(E.1)), E2 observed that all of these points featured long blue arcs on their left side (red solid box in Figure 3(E.1)), characteristic of densely populated urban areas. Following the government's "minimize resident impact" policy, E2 elevated noise sensitivity to a core criterion and demoted Site 7050 and Site 7055 from ranks 1 and 2 to 9 and 10, respectively (their "Current" values read 1 and 2, now physically located at the 9th and 10th rows of the table). Given that Site 7046 is superior to Site 7045 in terms of safety, Site 7046 (red dashed box in Figure 3(E.2)) was promoted to the first place. The final ranking is shown in the red solid box at the bottom right corner of Figure 3(E.2): sites are ordered from top to bottom, and this vertical sequence represents the ultimate ranks.

E2 confirmed geographical suitability in the 3D View and adjusted final rankings. After confirming the geographical suitability of the top-ranked Site 7046 in the 3D View (Figure 3(C.2)), E2 locked the adjustment using the "Save Rank" and "Apply Weight Scheme" function.

E2 verified the final site selection rationality in the Solution View. Within the Solution View (Figure 3(F)), E2 reviewed the ultimate choices for all clusters simultaneously. The radar chart of Solution 1 (red dashed box in Figure 3(F)) indicated that the automatically selected candidate site excels in both demand and accessibility while maintaining low noise sensitivity (all scores $>$ 80), represented by the thickest red line in the chart. This outcome perfectly aligned with E2's comprehensive objectives, confirming the validity of the decision-making approach. By clicking on different radar charts, E2 could visually inspect the spatial distribution of each final candidate on the map, ensuring that it meets overall regional-planning requirements.

B. Expert Interviews

Interview Process. To assess the system's practical applicability and effectiveness, we conducted interviews with four domain experts (E1–E4). Among them, E1–E3 are the three experts introduced in Section III-A, while E4—who was not involved in the design process—is a front-line engineer in eVTOL industry, specializing in vertiport construction planning. Initially, we provided them with a brief introduction to the system's functionality and design philosophy, highlighting the interactive features of the key views. The experts then engaged in a 30-minute hands-on session with guided instructions. Given their varying familiarity with visual analytics systems, we adopted a step-by-step approach to ensure they could fully understand each module. The interviews followed a semi-structured format, with each session lasting approximately 25 minutes. During these sessions, we documented their feedback on system usage and gathered suggestions for improvement.

System Evaluation. The experts unanimously acknowledged the system as a valuable decision-support tool for siting low-altitude transportation facilities. E1 remarked, "Traditional site selection methods rely heavily on extensive manual research and expert judgment, whereas this system significantly enhances efficiency through visual analytics that integrate multi-source data." E3 specifically praised the practicality of the 3D safety assessment module, stating, "The system translates complex parameters such as airspace restrictions and landing performance into intuitive visualizations, which greatly support real-world planning tasks." E2 agreed that the

Change View effectively addresses the challenge of evaluating multi-dimensional indicators in an innovative way. E4 stressed the operational perspective: "The 3-D clearance visualization immediately shows me where approach surfaces are blocked by buildings; this saves several rounds of on-site verification and significantly reduces construction-risk uncertainty."

User Experience. After familiarizing themselves with the basic operations, the experts were able to seamlessly utilize the core system functions. E1 remarked, "The linked design between the Spatial View and the 3D View effectively illustrates the spatial relationships among siting factors." E2 specifically highlighted, "Incorporating more detailed land-use indicators would greatly improve land coordination efficiency in practical planning scenarios." E3 noted that the interaction logic of the Ranking View could be further optimized to improve usability for non-expert users.E4 added that the radar-chart summary in the Solution View helped him "quickly communicate the trade-offs to project investors who are not GIS experts, which is critical for securing early-stage funding."

Improvement Suggestions. The experts provided several insightful recommendations for enhancement: (1) At the data level, incorporating additional government platform data (e.g., land-use characteristics); (2) At the functional level, adding modules for construction cost estimation and operational benefit prediction; (3) In terms of interaction design, streamlining workflows for advanced features.

C. User Study

To evaluate the usability of *VISTA* from the perspective of its target users, we conducted a user study with 10 participants. The study assessed three dimensions—system workflow, visual design and interaction, and system usability—through task-based evaluation and standardized questionnaires. Given the modest sample size, quantitative results should be interpreted as indicative of usability within the target user group; qualitative and behavioral findings additionally reveal directions for continued system refinement.

1) Study Design:

a) Questionnaire Design: We employed a combination of an adapted System Usability Scale (SUS) and custom-designed questions, comprising 12 items rated on a 7-point Likert scale (1 = "Strongly Disagree", 7 = "Strongly Agree"). As shown in Table I, the questionnaire covers three dimensions: System Workflow (Q1–Q5), Visual Design and Interaction (Q6–Q9), and System Usability (Q10–Q12). Specific items included "I can quickly locate clusters of candidate points of interest" (spatial cognition), "I can understand how the ranking algorithm prioritizes candidate locations" (algorithm transparency), and "The ranking view and change view help me adjust rankings quickly" (interaction efficiency).

b) Participants: We recruited 10 graduate students from the local university's transportation engineering department (4 females, 6 males, mean age 25.3 $\pm$ 1.7 years). All participants possessed foundational backgrounds in Geographic Information Systems (GIS) and Multi-Criteria Decision Analysis (MCDA) (8 master's students, 2 doctoral students), and all had conducted research on eVTOL siting or low-altitude traffic. While this ensured professional task comprehension, the sample reflects a technically trained user group; the usability ratings reported below should therefore be interpreted within this context. Future research with a broader range of stakeholders (e.g., urban planners, government officials) would complement these findings.

2) Tasks and Procedure:

a) Experimental Tasks: Participants completed three typical siting scenario tasks:

- **Task 1: Global Demand Assessment.** Based on the global heatmap and cluster glyphs, describe city-level demand distribution and identify 3 high-demand areas. *Observation focus:* Whether participants prioritized using heatmap layer controls (association between color depth and demand intensity) or size/density cues of cluster glyphs for spatial scanning.
- **Task 2: Site Ranking and Safety Verification.** Compare multi-dimensional characteristics of 3 candidate sites; verify building clearance requirements in the 3D view; adjust and save weighting schemes. *Observation focus:* Recording the switching path from cluster view $\rightarrow$ 3D view $\rightarrow$ ranking view; observing whether participants immediately checked the change view feedback when adjusting weights.
- **Task 3: Scenario Comparison and Trade-off Analysis.** Utilize t-SNE scatter plots to identify ranking fluctuation clusters, explain indicator differences, and manually adjust site rankings. *Observation focus:* Analyzing how participants coordinately used scatter plots (cluster selection) and bar charts (indicator comparison) for trade-off decision-making.

b) Experimental Procedure: The session began with a 10-minute background introduction (urban low-altitude traffic, *VISTA* framework, five evaluation indicators), followed by a 15-minute system demonstration (six views and interaction logic). Participants then independently operated the system for 30 minutes to complete the tasks, while experimenters observed their interaction behavior and collected verbal comments. Upon completion, participants filled out the aforementioned questionnaire.

3) Results and Analysis:

a) Questionnaire Results: The results of the questionnaire are shown in Figure 8. The overall questionnaire mean was 5.24 (SD = 0.28), indicating positive participant evaluations of *VISTA*. Dimension scores were as follows:

System Workflow (Mean = 5.08, SD = 0.13): Participants could locate high-demand clusters within an average of 2.8 minutes and expressed satisfaction with the immediate feedback of "drag-and-drop weight adjustment." However, algorithm explainability (Q5, Mean = 4.9) and weight adjustment feedback consistency (Q3, Mean = 5.0, SD = 0.89) scored notably lower than other items, indicating divergent user understanding of LambdaMART ranking logic and poor perceived consistency in score changes following weight adjustments.

Visual Design and Interaction (Mean = 5.50, SD = 0.35): This dimension performed best, with "The six main views

TABLE I
QUESTIONNAIRE ITEMS GROUPED BY EVALUATION DIMENSION

Dimension	Item
System Workflow	Q1. I can quickly locate candidate point clusters or candidate sites of interest, and utilize multi-dimensional data (e.g., demand, safety, cost) to support a comprehensive site-selection evaluation. Q2. I can use the system's 3-D analysis function to identify and avoid potential safety risks. Q3. I can explore how the multi-criteria scores of candidate sites change after adjusting the weights. Q4. The system can generate diverse site-selection schemes for me to choose and compare. Q5. I can understand how the ranking algorithm determines the priority of candidate sites.
Visual Design and Interaction	Q6. The spatial view provides a good design to display data at the global, cluster, and candidate-point levels. Q7. The 3-D view provides a good design to examine the safety of candidate sites. Q8. The ranking view and the change view help me quickly adjust the ranking and observe ranking changes. Q9. The six views (statistics, spatial, 3-D, ranking, change, solution) are intuitive and easy to use.
System Usability	Q10. The system provides sufficient information and tools to help me complete site selection. Q11. The system's interaction and operation logic align with my expectations. Q12. The system interaction is beginner-friendly, simple and easy to use.

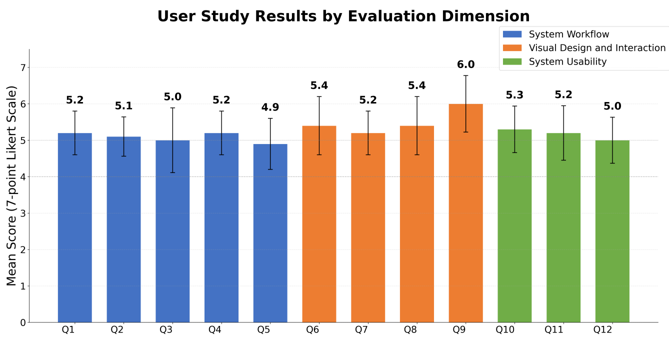

Fig. 8. Mean scores for 12 questionnaire items across three evaluation dimensions (System Workflow, Visual Design and Interaction, System Usability) on a 7-point Likert scale. Error bars represent ±1 SD. Higher scores indicate better perceived performance.

(Statistics, Spatial, 3D, Ranking, Change, Solution) are well-designed" (Q9) receiving the highest rating (Mean = 6.0). Radar charts and semi-transparent 3D building overlays were praised for "intuitively presenting airspace conflicts." Notably, the spatial view design (Q6, SD = 0.80) and ranking view (Q8, SD = 0.80) exhibited larger standard deviations, suggesting some users may have experienced difficulties processing complex spatial information or multi-dimensional ranking changes.

System Usability (Mean = 5.17, SD = 0.15): Novice friendliness (Q12, Mean = 5.0) received the lowest score within this dimension, followed by interaction logic rationality (Q11, Mean = 5.2). This suggests that while interaction logic is moderately acceptable, the system lacks sufficient support for first-time users, indicating a need for better onboarding guidance.

b) Interface Selection and Behavioral Correlation Analysis: Through observation of associations between user operation paths and questionnaire scores, we identified the following behavioral patterns:

1) **View Switching Strategy and Task Efficiency:** Efficient users (task completion time < 25 minutes) tended to adopt a linear path of "heatmap $\rightarrow$ cluster glyphs $\rightarrow$ ranking view" with minimal backtracking; inefficient users frequently switched between the 3D view and ranking view, possibly stemming from cognitive disconnect between 3D safety verification (Q2, Mean = 5.1) and ranking adjustment. This is consistent with the moderate scores and higher variance observed for Q2 (3D view-related) and Q8 (ranking view-related), suggesting that users had not yet established a coherent workflow integrating 3D verification with weight adjustment.
2) **Feedback Dependence in Weight Adjustment Behavior:** Participants with higher Q3 scores (≥ 6) generally exhibited iterative "adjust-observe-readjust" behaviors, frequently consulting the change view to verify weight impacts; those with lower Q3 scores (≤ 4) tended to adjust weights once and proceed directly to the next task without fully utilizing change view feedback. This indicates that while the Change View's feedback mechanism was functionally complete, its role in the analysis workflow was not spontaneously discovered by all participants.
3) **Algorithm Trust and Explanation Needs:** Participants with low Q5 scores (≤ 4, $n = 3$) exhibited "verification clicking" behaviors during tasks—repeatedly switching between different views to manually validate ranking rationality rather than relying on system outputs. This pattern suggests that when ranking rationale is not directly visible, some users attempt to reconstruct it through cross-view exploration.

c) Qualitative Feedback: One participant noted: "When using 2D GIS for siting previously, I needed to switch between CAD and regulatory documents; now I can see integrated results for height, noise, and cost with one click." Three participants suggested adding real-time meteorological interfaces and construction cost estimation modules; these features, while beyond the scope of the current prototype, represent valuable directions for future system iterations.

VIII. Discussion and Limitation

While *VISTA* offers an effective approach to eVTOL vertiport siting, our study reveals several limitations that point to valuable future research directions.

Data Limitations. The system currently relies on static datasets, limiting its responsiveness to real-time operational conditions. Future work will integrate real-time data streams (e.g., dynamic demand patterns, meteorological conditions) and richer eVTOL performance models to enable more precise, scenario-specific safety screening and planning.

Algorithmic Limitations. The current prototype employs a static weighting pipeline and processes 3D building data offline. Future versions will explore real-time obstacle-data integration and more adaptive ranking strategies that respond to dynamic urban conditions.

Evaluation Limitations. The evaluation, while providing initial evidence of VISTA's usability, was conducted with a limited sample of 4 domain experts and 10 technically trained students. The absence of non-expert stakeholders and the use of simulated rather than real-world planning tasks limit the generalizability of the findings. Future studies should incorporate diverse user groups and long-term deployment in operational planning environments.

Design Implications from User Study. Beyond these general limitations, the user study (Section VII-C) revealed specific interface-level insights. Participants with lower algorithm transparency scores tended to validate rankings manually across multiple views, pointing to the potential value of lightweight ranking explanations for building user trust. The limited spontaneous discovery of Change View feedback further indicates that surfacing ranking-change indicators more prominently within the Ranking View could improve feedback utilization. These refinements represent concrete directions for enhancing *VISTA*'s support for transparent, user-driven decision-making.

IX. Conclusion and Future Work

This paper introduces *VISTA*, a visual analytics framework that addresses the challenge of eVTOL vertiport siting by integrating multi-criteria decision-making, 3D spatial analysis, and interactive visualization. The system identifies potential sites through demand clustering and 3D safety screening, and incorporates ranking models that support dynamic weight adjustment. Our evaluation encompassed two case studies, four expert interviews, and a user study, confirming *VISTA*'s usability and effectiveness for technically trained users while also surfacing concrete directions for continued refinement. Future work includes integrating real-time data streams for dynamic planning, extending the evaluation to long-term deployment scenarios, and broadening the framework to other urban airspace environments.

X. Acknowledgments

This work is supported by grants from National Natural Science Foundation of China (No. 62302531), and Science and Technology Planning Project of Guangdong Province (No. 2023B1212060029).

References

[1] S. Rajendran and S. Srinivas, "Air taxi service for urban mobility: A critical review of recent developments, future challenges, and opportunities," *Transportation Research Part E: Logistics and Transportation Review*, vol. 143, p. 102090, 2020.

[2] H. Shon, S. Kim, and J. Lee, "Optimal planning of urban air mobility systems accounting for ground access trips," *International Journal of Sustainable Transportation*, vol. 18, no. 4, pp. 356–378, 2024.

[3] W. Kai, A. Jacquillat, and V. Vaze, "Vertiport planning for urban aerial mobility: An adaptive discretization approach," *Manufacturing & Service Operations Management*, vol. 24, no. 6, pp. 3215–3235, 2022.

[4] X. Jiang, S. Cao, B. Mo, J. Cao, H. Yang, Y. Tang, M. Hansen, J. Zhao, and R. Sengupta, "Simulation-based optimization for vertiport location selection: A surrogate model with machine learning method," *Transportation Research Record*, p. 03611981241277755, 2024.

[5] C. Guo, J. Nie, X. Hang, Y. Wang, Y. Chen, and D. Delahaye, "Vtol site location considering obstacle clearance during approach and departure," *Communications in Transportation Research*, vol. 4, p. 100118, 2024.

[6] D. Liu, D. Weng, Y. Li, J. Bao, Y. Zheng, H. Qu, and Y. Wu, "Smartadp: Visual analytics of large-scale taxi trajectories for selecting billboard locations," *IEEE Transactions on Visualization and Computer Graphics*, vol. 23, no. 1, pp. 1–10, 2016.

[7] D. Weng, H. Zhu, J. Bao, Y. Zheng, and Y. Wu, "Homefinder revisited: Finding ideal homes with reachability-centric multi-criteria decision making," in *Proceedings of the 2018 CHI Conference on Human Factors in Computing Systems*, 2018, pp. 1–12.

[8] L. Chen, H. Wang, Y. Ouyang, Y. Zhou, N. Wang, and Q. Li, "Fslens: A visual analytics approach to evaluating and optimizing the spatial layout of fire stations," *IEEE Transactions on Visualization and Computer Graphics*, 2023.

[9] A. Chakrabarty, V. Hosagrahara, and A. Lei, "Design of uam network and ecosystem integration," in *Proceedings of AIAA SCITECH 2024 Forum*, 2024, p. 0334.

[10] Q. Wei, Z. Gao, J.-P. Clarke, and U. Topcu, "Risk-aware urban air mobility network design with overflow redundancy," *Transportation Research Part B: Methodological*, vol. 185, p. 102967, 2024.

[11] Y. Zhao and T. Feng, "Strategic integration of vertiport planning in multimodal transportation for urban air mobility: A case study in beijing, china," *Journal of Cleaner Production*, vol. 467, p. 142988, 2024.

[12] K. Schweiger and L. Preis, "Urban air mobility: Systematic review of scientific publications and regulations for vertiport design and operations," *Drones*, vol. 6, no. 7, p. 179, 2022.

[13] M. Brunelli, C. C. Ditta, and M. N. Postorino, "New infrastructures for urban air mobility systems: A systematic review on vertiport location and capacity," *Journal of Air Transport Management*, vol. 112, p. 102460, 2023.

[14] D. N. Fadhil, "A gis-based analysis for selecting ground infrastructure locations for urban air mobility," *Inlangen. Master's Thesis, Technical University of Munich*, vol. 31, 2018.

[15] E. Feldhoff and G. Soares Roque, "Determining infrastructure requirements for an air taxi service at cologne bonn airport," *CEAS Aeronautical Journal*, vol. 12, no. 4, pp. 821–833, 2021.

[16] M. Rimjha, S. Hotle, A. Trani, N. Hinze, and J. C. Smith, "Urban air mobility demand estimation for airport access: A los angeles international airport case study," in *Proceedings of 2021 Integrated Communications Navigation and Surveillance Conference (ICNS)*. IEEE, 2021, pp. 1–15.

[17] K. H. Goodrich and B. Barmore, "Exploratory analysis of the airspace throughput and sensitivities of an urban air mobility system," in *Proceedings of 2018 Aviation Technology, Integration, and Operations Conference*, 2018, p. 3364.

[18] S. Rath and J. Y. Chow, "Air taxi skyport location problem with single-allocation choice-constrained elastic demand for airport access," *Journal of Air Transport Management*, vol. 105, p. 102294, 2022.

[19] B. German, M. Daskilewicz, T. K. Hamilton, and M. M. Warren, "Cargo delivery in by passenger evtol aircraft: A case study in the san francisco bay area," in *Proceedings of 2018 AIAA Aerospace Sciences Meeting*, 2018, p. 2006.

[20] C. Chin, K. Gopalakrishnan, H. Balakrishnan, M. Egorov, and A. Evans, "Efficient and fair traffic flow management for on-demand air mobility," *CEAS Aeronautical Journal*, pp. 1–11, 2021.

[21] K. Sheth, "Vamos! a regional modeling and simulation system for vertiport location assessment," in *Proceedings of AIAA AVIATION 2023 Forum*, 2023, p. 3412.

[22] V. Bulusu, E. B. Onat, R. Sengupta, P. Yedavalli, and J. Macfarlane, "A traffic demand analysis method for urban air mobility," *IEEE Transactions on Intelligent Transportation Systems*, vol. 22, no. 9, pp. 6039–6047, 2021.

[23] L. E. Alvarez, J. C. Jones, A. Bryan, and A. J. Weinert, "Demand and capacity modeling for advanced air mobility," in *Proceedings of AIAA Aviation 2021 Forum*, 2021, p. 2381.

[24] F. Naser, N. Peinecke, and B. I. Schuchardt, "Air taxis vs. taxicabs: A simulation study on the efficiency of uam," in *Proceedings of AIAA Aviation 2021 Forum*, 2021, p. 3202.

[25] M. Fu, R. Rothfeld, and C. Antoniou, "Exploring preferences for transportation modes in an urban air mobility environment: Munich case

study," *Transportation Research Record*, vol. 2673, no. 10, pp. 427–442, 2019.

[26] B. Rahman, R. Bridgelall, M. F. Habib, and D. Motuba, "Integrating urban air mobility into a public transit system: A gis-based approach to identify candidate locations for vertiports," *Vehicles*, vol. 5, no. 4, pp. 1803–1817, 2023.

[27] H. Shin, T. Lee, and H.-R. Lee, "Skyport location problem for urban air mobility system," *Computers & Operations Research*, vol. 138, p. 105611, 2022.

[28] M. Barsotti, Z. Gao, and J.-P. Clarke, "An eco-social approach to sustainable uam network design," in *Proceedings of AIAA AVIATION FORUM AND ASCEND 2024*, 2024, p. 3726.

[29] E. Lim and H. Hwang, "The selection of vertiport location for on-demand mobility and its application to seoul metro area," *International Journal of Aeronautical and Space Sciences*, vol. 20, pp. 260–272, 2019.

[30] J. Li, Y. Tian, T. Huang, and W. Gao, "Multi-task rank learning for visual saliency estimation," *IEEE Transactions on Circuits and Systems for Video Technology*, vol. 21, no. 5, pp. 623–636, 2011.

[31] T. Xie, Y. Ma, H. Tong, M. T. Thai, and R. Maciejewski, "Auditing the sensitivity of graph-based ranking with visual analytics," *IEEE Transactions on Visualization and Computer Graphics*, vol. 27, no. 2, pp. 1459–1469, 2020.

[32] H. U. Khan, F. Ali, M. Sohail, S. Nazir, and M. Arif, "Decision making for selection of smart vehicle transportation system using vikor approach," *International Journal of Data Science and Analytics*, pp. 1–15, 2024.

[33] B. Dy, N. Ibrahim, A. Poorthuis, and S. Joyce, "Improving visualization design for effective multi-objective decision making," *IEEE Transactions on Visualization and Computer Graphics*, vol. 28, no. 10, pp. 3405–3416, 2021.

[34] M. A. Khan and B. Mehran, "Hazardous materials facility siting optimization and ranking: A transportation risk mitigation framework," *PLoS One*, vol. 18, no. 11, p. e0290723, 2023.

[35] M. Scherr, "Multiple and coordinated views in information visualization," *Trends in information visualization*, vol. 38, pp. 1–33, 2008.

[36] D. Deng, W. Cui, X. Meng, M. Xu, Y. Liao, H. Zhang, and Y. Wu, "Revisiting the design patterns of composite visualizations," *IEEE Transactions on Visualization and Computer Graphics*, vol. 29, no. 12, pp. 5406–5421, 2022.

[37] Y. Zhang, L. Xu, S. Tao, Q. Guan, Q. Li, and H. Zeng, "Cslens: Towards better deploying charging stations via visual analytics——a coupled networks perspective," *IEEE Transactions on Visualization and Computer Graphics*, 2024.

[38] K. Zhang, H. Chen, H.-N. Dai, H. Liu, and Z. Lin, "Spovis: Decision support system for site selection of sports facilities in digital twinning cities," *IEEE Transactions on Industrial Informatics*, vol. 18, no. 2, pp. 1424–1434, FEB 2022.

[39] Q. Yu, D. Feng, G. Li, Q. Chen, and H. Zhang, "Advmob: Interactive visual analytic system of billboard advertising exposure analysis based on urban digital twin technique," *Advanced Engineering Informatics*, vol. 62, no. C, OCT 2024.

[40] D. Weng, R. Chen, Z. Deng, F. Wu, J. Chen, and Y. Wu, "Srvis: Towards better spatial integration in ranking visualization," *IEEE Transactions on Visualization and Computer Graphics*, vol. 25, no. 1, pp. 459–469, 2018.

[41] R. Pammi, S. Afzal, H. P. Dasari, M. Yousaf, S. Ghani, M. S. Venkatraman, and I. Hoteit, "A visual analytics framework for renewable energy profiling and resource planning," 2023.

[42] D. Karamshuk, A. Noulas, S. Scellato, V. Nicosia, and C. Mascolo, "Geo-spotting: mining online location-based services for optimal retail store placement," in *Proceedings of the ACM SIGKDD International Conference on Knowledge Discovery and Data Mining*, 2013, pp. 793–801.

[43] Y. Li, Y. Zheng, S. Ji, W. Wang, L. H. U, and Z. Gong, "Location selection for ambulance stations: a data-driven approach," in *Proceedings of the 23rd SIGSPATIAL International Conference on Advances in Geographic Information Systems*, 2015, pp. 1–4.

[44] S. Diehl, F. Beck, and M. Burch, "Uncovering strengths and weaknesses of radial visualizations—an empirical approach," *IEEE Transactions on Visualization and Computer Graphics*, vol. 16, no. 6, pp. 935–942, 2010.

[45] M. Waldner, A. Diehl, D. Gračanin, R. Splechtna, C. Delrieux, and K. Matković, "A comparison of radial and linear charts for visualizing daily patterns," *IEEE Transactions on Visualization and Computer Graphics*, vol. 26, no. 1, pp. 1033–1042, 2019.

[46] J. Zou, X. Zhang, Y. Cong, Z. Gao, and J. Shi, "Research and modeling of commercial location selection based on geographic big data and mobile signaling data-a case study of the central urban area of beijing," *ISPRS International Journal of Geo-Information*, vol. 13, no. 12, DEC 2024.

[47] N. Ferreira, M. Lage, H. Doraiswamy, H. Vo, L. Wilson, H. Werner, M. Park, and C. Silva, "Urbane: A 3d framework to support data driven decision making in urban development," in *Proceedings of 2015 IEEE conference on visual analytics science and technology (VAST)*. IEEE, 2015, pp. 97–104.

[48] R. Mota, N. Ferreira, J. D. Silva, M. Horga, M. Lage, L. Ceferino, U. Alim, E. Sharlin, and F. Miranda, "A comparison of spatiotemporal visualizations for 3d urban analytics," *IEEE Transactions on Visualization and Computer Graphics*, vol. 29, no. 1, pp. 1277–1287, 2023.

[49] M. Sedlmair, M. Meyer, and T. Munzner, "Design study methodology: Reflections from the trenches and the stacks," *IEEE Transactions on Visualization and Computer Graphics*, vol. 18, no. 12, pp. 2431–2440, 2012.

[50] J. Schulman, F. Wolski, P. Dhariwal, A. Radford, and O. Klimov, "Proximal policy optimization algorithms," *arXiv preprint arXiv:1707.06347*, 2017.

[51] M. of Civil Aviation of China, "Technical standards for civil helicopter airports (mh 5013—2023)," Ministry of Civil Aviation of China, Beijing, China, Tech. Rep., February 2023, replaces MH 5013—2014, implemented on April 1, 2023. [Online]. Available: http://www.caac.gov.cn/

[52] C. C. A. Association, "Technical requirements for electric vertical take-off and landing aircraft (evtol) landing fields (t/ccaatb 0062—2024)," China Civil Airport Association, Beijing, China, Tech. Rep., May 2024, implemented on June 22, 2024. [Online]. Available: http://www.ccaatb.org.cn/

[53] C. J. Burges, "From ranknet to lambdarank to lambdamart: An overview," *Learning*, vol. 11, no. 23-581, p. 81, 2010.

[54] M. Li, H. Wang, H. Long, J. Xiang, B. Wang, J. Xu, and J. Yang, "Community detection and visualization in complex network by the density-canopy-kmeans algorithm and mds embedding," *IEEE ACCESS*, vol. 7, pp. 120 616–120 625, 2019.

[55] C. Collins, G. Penn, and S. Carpendale, "Bubble sets: Revealing set relations with isocontours over existing visualizations," *IEEE Transactions on Visualization and Computer Graphics*, vol. 15, no. 6, pp. 1009–1016, 2009.

[56] K. Li, Y.-N. Li, H. Yin, Y. Hu, P. Ye, and C. Wang, "Visual analysis of retailing store location selection," in *Proceedings of the 12th International Symposium on Visual Information Communication and Interaction*, 2019, pp. 1–8.

[57] H. Qu, H. Wang, W. Cui, Y. Wu, and M.-Y. Chan, "Focus+ context route zooming and information overlay in 3d urban environments," *IEEE Transactions on Visualization and Computer Graphics*, vol. 15, no. 6, pp. 1547–1554, 2009.

[58] S. Gratzl, A. Lex, N. Gehlenborg, H. Pfister, and M. Streit, "Lineup: Visual analysis of multi-attribute rankings," *IEEE Transactions on Visualization and Computer Graphics*, vol. 19, no. 12, pp. 2277–2286, 2013.

[59] D. Liu, P. Xu, and L. Ren, "Tpflow: Progressive partition and multidimensional pattern extraction for large-scale spatio-temporal data analysis," *IEEE Transactions on Visualization and Computer Graphics*, vol. 25, no. 1, pp. 1–11, 2018.

[60] L. van der Maaten and G. Hinton, "visualizing data using t-sne," *Journal of Machine Learning Research*, vol. 9, pp. 2579–2605, 11 2008.

[61] S. Gu, Y. Dai, Z. Feng, Y. Wang, and H. Zeng, "T-pickseer: visual analysis of taxi pick-up point selection behavior," *Journal of Visualization*, vol. 27, no. 3, pp. 451–468, JUN 2024.

Haipeng Zeng is currently an associate professor in School of Intelligent Systems Engineering at Sun Yat-sen University (SYSU). He obtained his Ph.D. in Computer Science from the Hong Kong University of Science and Technology. His research interests include data visualization, visual analytics, machine learning and intelligent transportation. For more details, please refer to http://www.zenghp.org/.

Wei Huang is currently working towards the M.S. degree in the School of Intelligent Systems Engineering at Sun Yat-sen University. She received a B.S. degree in transportation engineering from Sun Yat-Sen University. Her research interests include low-altitude economy, visual analytics and transportation big data.

Xingyu Zhu is currently a senior undergraduate student in the School of Intelligent Systems Engineering at Sun Yat-sen University, majoring in intelligent transportation. Her research interests include transportation big data and visual analytics.

Yanqing Peng is currently a senior undergraduate student in the School of Intelligent Systems Engineering at Sun Yat-sen University, majoring in intelligent transportation. Her research interests include machine learning, visual analytics, and transportation big data.

Wenjie Shi is currently a senior undergraduate student in the School of Intelligent Systems Engineering at Sun Yat-sen University, majoring in Intelligent Transportation. His research interests lie in computer vision, pattern recognition, and human visual attention for autonomous systems.

Quan Li is currently a tenure-track assistant professor at School of Information Science and Technology, ShanghaiTech University. He received his Ph.D. from the Hong Kong University of Science and Technology. His research interests lie in visual analytics, interpretable machine learning, and human-computer interaction. For more details, please refer to https://faculty.sist.shanghaitech.edu.cn/liquan/.

Shaorui Zhou is currently an associate professor in School of Intelligent Systems Engineering at Sun Yat-sen University (SYSU). He received the Ph.D. degree in management from Sun Yat-sen University and City University of Hong Kong in 2015. His research interests include smart ports and shipping systems, low altitude economy, intelligent optimization algorithms, and operations management in big data environments.